

Valence ionization spectra of group six metal hexacarbonyls studied by the symmetry-adapted cluster-configuration interaction method

Ryoichi Fukuda,^{1,2,a)} Seigo Hayaki,² and Hiroshi Nakatsuji^{1,2}

¹Quantum Chemistry Research Institute, JST CREST, Kyodai Katsura Venture Plaza, North building, 36-1 Goryo Oohara, Nishikyo-ku, Kyoto 615-8245, Japan

²Department of Synthetic Chemistry and Biological Chemistry, Graduate School of Engineering, Kyoto University, Kyoto-Daigaku-Katsura, Nishikyo-ku, Kyoto 615-8510, Japan

(Received 6 March 2009; accepted 13 October 2009; published online 2 November 2009)

The valence ionization spectra up to 20 eV of group six metal carbonyls, chromium hexacarbonyl, molybdenum hexacarbonyl, and tungsten hexacarbonyl were studied by the symmetry-adapted cluster-configuration interaction (SAC-CI) method. The assignments of the spectra are given based on reliable SAC-CI calculations. The relativistic effects including the spin-orbit effects are important for the ionization spectrum of $W(CO)_6$. The relation between the metal-CO distance and ionization energies was examined. The lowest ionization energies of the three metal carbonyls are approximately the same because of the energy dependence of the metal-CO length and relativistic effects. In $Cr(CO)_6$, the Cr-CO interaction significantly increases the lowest ionization energy in comparison with $Mo(CO)_6$ and $W(CO)_6$ because of the relatively short metal-CO bond length. The relativistic effect reduces the lowest ionization energy of $W(CO)_6$ because the effective core potential of 5d electrons is more efficiently screened as a result of the relativistic contraction of the inner electrons. © 2009 American Institute of Physics. [doi:10.1063/1.3257963]

I. INTRODUCTION

Ionization spectra are important for studying the valence electronic structure of molecules and molecular systems because energy levels of electrons can be directly observed using spectroscopic techniques such as ultraviolet (UV) photoelectron spectroscopy¹ (PES) or Penning ionization electron spectroscopy (PIES).² Accurate assignment of peaks is necessary for extracting information about the electronic structure from the measured spectrum. Within the molecular orbital theory, Koopmans' theorem³ relates calculated orbital energies to observed ionization energies; therefore, theoretical computations are frequently used for assignment of ionization spectra. Although the simplicity of Koopmans' theorem is attractive, it is usually inaccurate for quantitative estimation. Additionally, Koopmans' theorem is invalid for systems such as transition metal compounds in which orbital relaxation is a significant contribution to the ionization process.^{4,5} Accurate theories, in which electron correlation and orbital relaxation are considered consistently, are essential for assigning the spectrum correctly and for obtaining much useful knowledge about the electronic structure by theoretical and spectroscopic methodologies. The symmetry-adapted cluster⁶ (SAC) /SAC-configuration interaction (SAC-CI) (Ref. 7) method used in the present study has such features.

The SAC/SAC-CI method is an electron-correlation theory for the ground, excited, electron-attached, and ionized states. The SAC-CI method has been applied to studying diverse aspects of chemistry, physics, and biology⁸ as well

as ionization spectra. The SAC-CI method has accurately described the ionization potential of molecules consisting of main group elements: organic molecules with π -conjugation,⁹ inorganic molecules,¹⁰ silicon compounds,¹¹ and hydrocarbon cages.¹² The SAC-CI general- R method¹³ has been applied to outer- and inner-valence ionization, including shake-up satellites.¹⁴ The highly accurate general- R method has achieved "fine theoretical spectroscopy" for the ionization of a series of molecules.^{15,16} In this study, we will report applications of the SAC-CI method to the ionization of transition metal compounds. Although some important results have been reported about transition metal compounds,^{5,17} we have not paid much attention to the couplings between electron correlation and orbital reorganization. For a systematic study of transition metal compounds, we need to establish the method of computations for systems in which electron correlation and orbital reorganization are significantly coupled. For this purpose, we will study the valence ionization spectra of group six metal carbonyls. In addition, relativistic effects could be important for this kind of study. The trends of group six metal carbonyls will be discussed in terms of the relativistic and other periodic effects.

Metal carbonyls are among the most typical compounds of transition metals; for sixth group elements, hexacarbonyls are well known. They have been widely studied as a prototype for understanding the chemical bonds of organometallic compounds^{18,19} or a model for adsorption of carbon monoxide on metal surfaces.²⁰ On the ionizations in the valence region, He I and He II PES,²¹ x-ray PES (XPES),²² synchrotron radiation PES (SRPES),^{23,24} and PIES (Ref. 25) have been reported for $Cr(CO)_6$, $Mo(CO)_6$, and $W(CO)_6$. The spectra have been analyzed using Koopmans' theorem or

^{a)}Electronic mail: fukuda@qcri.or.jp.

semiempirical DV X- α calculations.²⁶ Reliable *ab initio* calculations have been reported only for Cr(CO)₆ with the third-order algebraic diagrammatic construction scheme [ADC(3)].²⁷ Other *ab initio* results using outer-valence Green's function (OVGF) calculations have been reported for Mo(CO)₆ and W(CO)₆.²⁸ However, no systematic study using a reliable computational method has been reported for the three carbonyls. Previous assignments and arguments relied on the similarity of these three carbonyls.^{21,23–25} Indeed, their ionization spectra are very similar, even though the differences in ionization energies of the atoms are more than 1 eV between the group six metals.^{29,30} The lowest ionized state of these three carbonyls was studied by electron momentum spectroscopy and Hartree–Fock and density functional theory (DFT) calculations.³¹ The lowest states have metal valence d character and have very similar momentum profiles and electron density distributions. The reason for this similarity has not been clearly explained. If the reason is left unclear, this assumption of similarity seems to be too simple. A systematic study is necessary to provide reliable assignments for spectra of the three carbonyls and to discuss the periodic trends in their ionization.

The aim of the present study is to investigate the periodic trends of the valence ionization spectra of group six metal hexacarbonyls with reliable *ab initio* calculations. We performed the SAC-CI calculations for the valence ionization of Cr(CO)₆, Mo(CO)₆, and W(CO)₆ including spin-free relativistic and spin-orbit (SO) effects. The present calculations well reproduced the ionization energies observed experimentally using PES.^{21–24} A consistent assignment was provided for the experimentally identified peaks of the group six metal hexacarbonyls. This study is a typical example of the application of the SAC-CI method to transition metal compounds. A suitable computational condition is given for studying ionizations of transition metal compounds that requires consistent consideration of electron correlation and orbital relaxation; they are compactly described by unlinked terms in the SAC-CI method. The metal-carbonyls interaction was studied in terms of the ionization energies. The dependence of ionization energies on the metal-carbonyl bond length was shown and the ionization energies were sensitive to the bond length for the states that have ionization character from metal-carbonyl bonding orbitals. The relativistic effect on the ionization energies was examined and its importance for W(CO)₆ was shown. The similarity in the ionization energies of these carbonyls was explained by the interaction between the metal and carbonyls and the relativistic effect.

II. METHOD OF CALCULATIONS

The SAC/SAC-CI calculations were carried out with the direct SAC-CI program,³² which has been incorporated into the GAUSSIAN development version.³³ The direct SAC-CI is a new computational algorithm for the SAC-CI singles and doubles (SD)-R method, which has improved the efficiency and accuracy by using the direct CI-like algorithm that is combined with the perturbation-selection technique. The

SAC method describes the neutral ground state by the cluster expansion with the symmetry-adapted excitation operators $\{S_i^\dagger\}$ as

$$\Psi_{\text{SAC}} = \exp\left(\sum_I c_I S_I^\dagger\right)|0\rangle, \quad (1)$$

where $|0\rangle$ is the closed-shell Hartree–Fock determinant. With the SAC-CI method, ionized states are formed by acting the ionization operators $\{R_i^\dagger\}$ on the SAC wave function as

$$\Psi_{\text{SAC-CI}} = \sum_I d_I R_I^\dagger |\Psi_{\text{SAC}}\rangle. \quad (2)$$

We have used the SD SAC/SAC-CI method in which single and double excitations are included in the S and R operators.

In the present study, we considered the unlinked terms that include S_1 operators in addition to the default unlinked terms;³⁴ here S_1 and S_2 denote the singles and doubles in $\{S_i^\dagger\}$, respectively. In particular, we included $\langle S_1|H|S_1S_1\rangle$, $\langle S_1|H|S_1S_2\rangle$, $\langle S_2|H|S_1S_1\rangle$, $\langle S_2|H|S_1S_2\rangle$, and $\langle S_2|H|S_2S_2\rangle$ for solving the SAC equations and included $\langle R_1|H|R_1S_1\rangle$, $\langle R_1|H|R_1S_2\rangle$, $\langle R_1|H|R_2S_1\rangle$, $\langle R_2|H|R_1S_1\rangle$, $\langle R_2|H|R_1S_2\rangle$, and $\langle R_2|H|R_2S_2\rangle$ for the SAC-CI secular equations. These additional terms, which are not included in the default calculations, are usually negligible for computations of molecules consisting of main group elements because the coefficients of the S_1 operators are sufficiently small. For transition metal compounds, orbital reorganization of the SAC wave function, which is described by S_1 , is significantly coupled with the electron correlation. Thus, these additional terms greatly affect the ionization energies of d electrons of transition metal compounds.

The relativistic effect was considered using the second-order Douglas–Kroll–Hess quasirelativistic Hamiltonian.³⁵ The scalar-relativistic Hamiltonian was used for the Hartree–Fock and SAC/SAC-CI calculations. The SO effect was calculated by diagonalizing the SO Hamiltonian matrix consisting of the SAC-CI solutions. Details of the SO effect based on the SAC-CI solution are available.¹²

Ahlrichs' [6s3p3d] basis³⁶ was used for Cr with augmented p- and f-type functions. The augmented p-functions with the exponents $\alpha(p)=0.1666$ and 0.0617 were generated by extrapolation of the outermost functions. The exponent of the f-function, $\alpha(f)=0.537\ 619$, was taken from the d-function. For Mo and W, Dyal's relativistic large-component sets were used with segment contraction.^{37,38} One f-function was added for Mo with $\alpha(f)=0.351\ 157\ 7$ taken from the d-function. The final form of the basis functions was [6s5p3d1f], [8s7p5d1f], and [10s9p7d2f] for Cr, Mo, and W. The D95 basis³⁹ was used for C and O. The equilibrium geometries of the coupled-cluster singles doubles with perturbative triples [CCSD(T)] method with the above basis were used for the SAC-CI calculations. We assumed that the correction for triples was necessary for an appropriate description of the metal-carbonyl distances because the T_1 amplitudes were not small. All of the molecules have O_h point group symmetry. The bond distances for the present calculations are summarized in Table I. The M–C lengths in the present study were longer than the MP2 (second-order Møller–Plesset perturbation theory) values⁴⁰ and were similar

TABLE I. Theoretical and experimental bond lengths (angstrom).

Method	Cr(CO) ₆		Mo(CO) ₆		W(CO) ₆	
	M–C	C–O	M–C	C–O	M–C	C–O
This work	1.895	1.187	2.080	1.190	2.100	1.190
MP2 ^a	1.861	1.168	2.061	1.164	2.060	1.166
GGA ^b	1.904	1.156	2.079	1.155	2.106	1.155
B3LYP ^c	1.920	1.139	2.084	1.139	2.071	1.141
mPW1PW91 ^d			2.057	1.136	2.056	1.138
Expt	1.941 ^e	1.140 ^e	2.063 ^f	1.145 ^f	2.058 ^f	1.148 ^f
	1.916 ^g	1.140 ^g	2.059 ^h	1.145 ^h		

^aReference 40.^bReference 41.^cReference 42.^dReference 28 (basis CN).^eNeutron diffraction, Ref. 43.^fElectron diffraction, Ref. 45^gX-ray, Ref. 42.^hX-ray, Ref. 46.

to the DFT values^{28,41,42} and experimental results.^{43–46} The C–O lengths in the present study were longer than the other theoretical and experimental values. We will discuss the effects of bond lengths on the ionization energies.

The 1s electrons of carbonyls and the largest noble gas core electrons were excluded for the SAC/SAC-CI calculations using the frozen core approximation; the cores were Ar, Kr, and Xe for Cr, Mo, and W, respectively. The perturbation selection technique⁴⁷ was used for the SAC/SAC-CI calculation; the thresholds for the ground and ionized states were set to $\lambda_g = \lambda_e = 1.0E-7$. The ionization cross sections were calculated by the monopole approximation.⁴⁸ They are a rough estimation of the relative intensities of peaks because the monopole approximation is valid for high energy limit and is insufficient to reproduce the intensity of UV PES. The SAC-CI theoretical spectra were convoluted with a Gaussian

envelope to simulate the Frank–Condon width and the resolution of the spectrometer; the full width at half maximum (FWHM) of the Gaussian was set to 0.2 eV.

III. RESULTS AND DISCUSSION

A. Ionization spectra

Tables II–IV show the ionization energies and the orbital character of the dominant configurations for Cr(CO)₆, Mo(CO)₆, and W(CO)₆ calculated with the SAC-CI method, respectively. The SAC-CI results without and with SO are shown. Other theoretical results by Koopmans' theorem, ADC(3),²⁷ OVGf,²⁸ and pseudospectral Dirac–Kohn–Sham (DKS) (Ref. 49) and experimental ionization energies by He I PES,²¹ SRPES,^{23,24} and XPES (Ref. 22) are also given

TABLE II. Ionization energies (eV) and ionizing orbital character for Cr(CO)₆.

State	Character	Theory (without SO)			Theory (with SO)		Experiment		
		KT ^a	ADC ^b	SAC-CI ^c	State ^d	SAC-CI	He I PES ^e	XPES ^f	
1 ² T _{2g}	Cr(3d)+CO(π^*)	10.42	9.15(0.90)	8.58(0.90)	1E _{5/2} ⁺ 1G _{3/2} ⁺	8.55 8.59	8.40	A	8.4
1 ² T _{1u}	CO(5 σ)+Cr(4p)	16.63	14.06(0.79)	13.77(0.88)	1G _{3/2} ⁺ 1E _{1/2} ⁺	13.76 13.78	13.38	B ₁	13.5
1 ² T _{1g}	CO(1 π)	17.28	14.75(0.57)	14.59(0.84)	2G _{3/2} ⁺ 1E _{1/2} ⁺	14.58 14.60	14.21	B ₂	14.3
1 ² E _g	CO(5 σ)+Cr(3d)	17.55	14.79(0.54), 15.14(0.19)	14.81(0.88)	3G _{3/2} ⁺	14.81			
1 ² T _{2u}	CO(1 π)	17.52	14.94(0.59)	14.84(0.83)	1E _{5/2} ⁻ 2G _{3/2} ⁻	14.83 14.85	14.40	B ₃	
2 ² T _{2g}	CO(1 π)	18.30	15.71(0.39)	15.48(0.84)	2E _{5/2} ⁺ 4G _{3/2} ⁺	15.47 15.48	15.12	B ₅	
2 ² T _{1u}	CO(1 π)	18.41	15.51(0.57)	15.49(0.82)	3G _{3/2} ⁻ 2E _{1/2} ⁻	15.48 15.51			
1 ² A _{1g}	CO(5 σ)+Cr(4s)	19.93	16.77(0.70)	16.19(0.85)	2E _{1/2} ⁺	16.19	15.60	B ₆	15.8
2 ² E _g	CO(4 σ)	22.19	18.79(0.29), 19.00(0.32)	18.06(0.84)	5G _{3/2} ⁺	18.06	17.82	C ₁	17.9
3 ² T _{1u}	CO(4 σ)	23.39	18.88(0.35), 19.01(0.33)	18.29(0.84)	4G _{3/2} ⁺ 3E _{1/2} ⁺	18.24 18.26			
2 ² A _{1g}	CO(4 σ)+Cr(4s)	24.26	20.02(0.59)	19.90(0.69)	3E _{1/2} ⁺	19.90	19.7	C ₂	20

^aKoopmans' theorem, this work.^bADC(3) results with large pole strength (given in parentheses), Ref. 27.^cPole strengths are given in parentheses.^dDouble group representation.^eReference 21.^fReference 22.

TABLE III. Ionization energies (eV) and ionizing orbital character for Mo(CO)₆.

State	Character	Theory (without SO)				Theory (with SO)		Experiment		
		KT ^a	OVGF ^b	TDA ^c	SAC-CI ^d	State ^e	SAC-CI	He I PES ^f	SRPES ^g	
1 ² T _{2g}	Mo(4d)+CO(π*)	9.63	8.14	7.86	8.47(0.92)	1E _{5/2} ⁺	8.41	8.50	A	
						1G _{3/2} ⁺	8.49			
1 ² T _{1u}	CO(5σ)+Mo(5p)	16.64	13.88	13.40, 13.72	13.60(0.86)	1G _{3/2} ⁻	13.55	13.32	B ₁	12.7–13.8
						1E _{1/2} ⁻	13.67			
1 ² T _{1g}	CO(1π)	17.34	15.52	14.17	14.46(0.80)	2G _{3/2} ⁺	14.45	14.18	B ₂	13.83–14.47
						1E _{1/2} ⁺	14.47			
1 ² T _{2u}	CO(1π)	17.51	15.64	14.62, 14.63	14.62(0.79)	1E _{5/2} ⁻	14.61	14.4	B ₃	
						2G _{3/2} ⁻	14.62			
2 ² T _{1u}	CO(1π)	17.89	15.86	15.00	14.93(0.80)	3G _{3/2} ⁻	14.91	14.66	B ₄	14.50–15.14
						2E _{1/2} ⁻	14.97			
2 ² T _{2g}	CO(1π)	18.04	16.13	15.39, 15.40	15.06(0.85)	2E _{5/2} ⁺	15.05	15.2	B ₅	
						3G _{3/2} ⁺	15.07			
1 ² E _g	CO(5σ)+Mo(4d)	18.25	15.45	15.64	15.10(0.78)	4G _{3/2} ⁺	15.10			
1 ² A _{1g}	CO(5σ)+Mo(5s)	19.40			15.65(0.83)	2E _{1/2} ⁺	15.65	15.6	B ₆	15.17–16.60
3 ² T _{1u}	CO(4σ)	22.27			17.97(0.82)	4G _{3/2} ⁻	17.96	17.70	C ₁	
						3E _{1/2} ⁻	18.00			
2 ² E _g	CO(4σ)	22.41			18.03(0.82)	5G _{3/2} ⁻	18.03			
2 ² A _{1g}	CO(4σ)+Mo(5s)	23.35			18.94(0.80)	3E _{1/2} ⁺	18.94			
								19.7	C ₂	

^aKoopmans' theorem, this work.^bReference 28, pole strengths exceed 0.8.^cOnly the ionization energies were taken from Ref. 28 (see text).^dPole strengths are given in parentheses.^eDouble group representation.^fReference 21.^gReference 23.

in the Tables. The comparisons between the calculated spectrum and He I PES (Ref. 21) are shown in Figs. 1–3.

In the SAC-CI coefficients, one-electron ionization configurations were dominant for these states. This may appear

to be contradicting the ADC(3) results in which the quasiparticle picture was significantly broken down with large mixing of two-hole-one-particle (2h1p) configurations for several states.²⁷ For the 1T_{2g}, 4E_g, and 6T_{1u} states of Cr(CO)₆, the

TABLE IV. Ionization energies (eV) and ionizing orbital character for W(CO)₆.

State	Character	Theory (without SO)				Theory (with SO)			Experiment		
		KT ^a	OVGF ^b	TDA ^c	SAC-CI ^d	State ^e	DKS ^f	SAC-CI	He I PES ^g	SRPES ^h	
1 ² T _{2g}	W(5d)+CO(π*)	9.38	8.1	7.77	8.29(0.93)	1E _{5/2} ⁺	8.30	8.14	8.30	A	
						1G _{3/2} ⁺	8.53	8.37	8.56		8.57
1 ² T _{1u}	CO(5σ)+W(6p)	16.76	14.03	13.49, 13.54	13.64(0.87)	1G _{3/2} ⁻	13.13	13.28	13.27	B ₁	13.38
						1E _{1/2} ⁻	13.58	14.11			
1 ² T _{1g}	CO(1π)	17.36	15.42	14.06	14.39(0.79)	2G _{3/2} ⁺	14.51	14.38	14.20	B ₂	14.21
						1E _{1/2} ⁺	14.53	14.39			
1 ² T _{2u}	CO(1π)	17.52	15.55	14.50	14.59(0.78)	1E _{5/2} ⁻	14.65	14.53	14.42	B ₃	
						2G _{3/2} ⁻	14.66	14.53			
2 ² T _{1u}	CO(1π)	17.92	15.80	14.74	14.86(0.79)	3G _{3/2} ⁻	14.84	14.76	14.88	B ₄	14.83
						2E _{1/2} ⁻	14.95	15.21			
2 ² T _{2g}	CO(1π)	18.04	16.04	14.94	14.99(0.78)	2E _{5/2} ⁺	15.06	14.97	15.2	B ₅	15.42
						3G _{3/2} ⁺	15.08	14.99			
1 ² E _g	CO(5σ)+W(5d)	18.45	15.71	15.08	15.11(0.85)	4G _{3/2} ⁺	14.94	15.11			
1 ² A _{1g}	CO(5σ)+W(6s)	19.75		15.33	15.88(0.82)	2E _{1/2} ⁺	15.74	15.88	15.54	B ₆	
3 ² T _{1u}	CO(4σ)	22.28		15.84	17.94(0.82)	4G _{3/2} ⁻		17.83	17.84	C ₁	17.63
						3E _{1/2} ⁻		18.25			
2 ² E _g	CO(4σ)	22.46			18.16(0.81)	5G _{3/2} ⁺		18.16			18.06
2 ² A _{1g}	CO(4σ)+W(6s)	23.71			19.25(0.79)	3E _{1/2} ⁺		19.25			18.52
									20.2	C ₂	20.06

^aKoopmans' theorem, this work.^bReference 28, pole strengths exceed 0.8.^cOnly the ionization energies were taken from Ref. 28 (see text).^dPole strengths are given in parentheses.^eDouble group representation.^fReference 49. Values are shifted by +1.5426 eV.^gReference 21.^hReference 24.

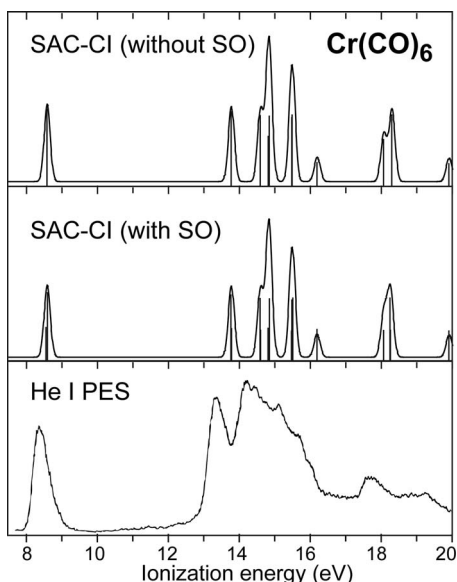


FIG. 1. Valence ionization spectra of chromium hexacarbonyl by the SAC-CI method and He I PES (Ref. 21).

distinction between the main line and satellite line was meaningless in the ADC(3) result. In this study, we calculated the satellite states, in which $2h1p$ is the dominant configurations, by the SAC-CI SD-R method. The results are summarized in Table V and they are discussed in the following section. As a result, such satellite states have little effect on the shapes of main peaks and the assignment less than 19 eV. Here, we discuss about the states in which one-electron ionization configurations were dominant. In these states the coefficient of the main one-hole configuration was about 0.9 and coefficients for $2h1p$ configurations were less than 0.2. Although one-electron ionization from neutral SAC state is dominant for 1^2T_{2g} state, the ionization energies by Koopmans' theorem are significantly deviated from the observations and the SAC-CI results. The similarity of the first

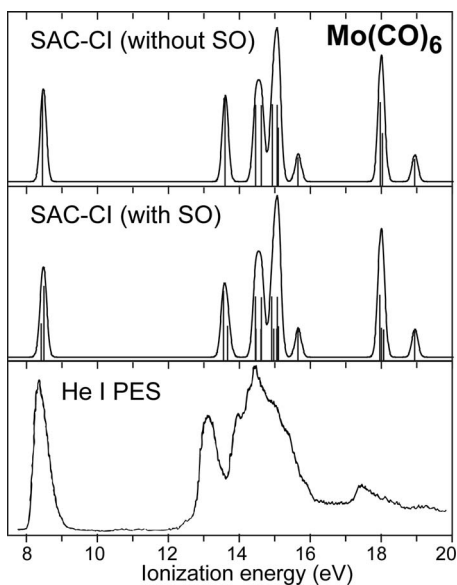


FIG. 2. Valence ionization spectra of molybdenum hexacarbonyl by the SAC-CI method and He I PES (Ref. 21).

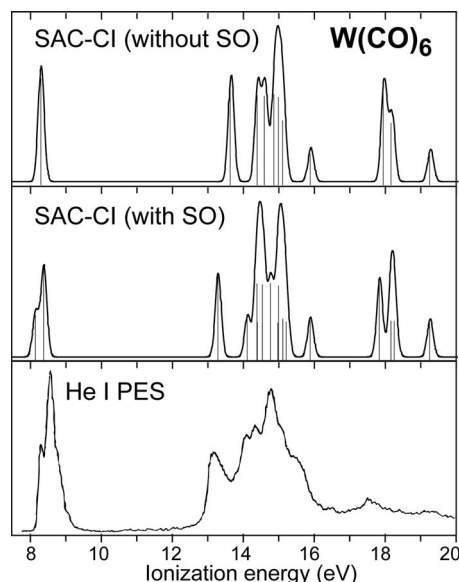


FIG. 3. Valence ionization spectra of tungsten hexacarbonyl by the SAC-CI method and He I PES (Ref. 21).

ionization energies could not be explained by Koopmans' theorem. The energy differences of the 1^2T_{2g} states of the three carbonyls were more than 1 eV by Koopmans' theorem. This was too large in comparison with the experimental findings.

The SAC-CI method well reproduced the overall trends of the experimental findings. The qualitative agreement with experimental ionization energies was better than those by other theoretical calculations; in particular, the first ionizations were well described by the SAC-CI method for the three carbonyls. Other peaks were calculated about 0.2–0.4 eV higher than the experimental observations. This deviation would be corrected by improving the basis sets of the carbonyls. The ADC(3) includes single-hole and $2h1p$ configurations and diagonalizes the Hamiltonian matrix to obtain the ionization energies and pole strengths. The methodology is similar to the SAC-CI SD-R. Therefore, both the methods would provide similar results at least for main peaks. The difference between the SAC-CI and ADC(3) results must be due to the computational conditions; the number of active virtual orbitals taken into account in Ref. 27 was too small. The OVGf method is based on the perturbation theory; therefore, the SAC-CI is theoretically superior in particular for higher energy region. Molecular geometries also affect on the ionization energies. Energies of some states are sensitive to metal-CO bond length. This point will be discussed in the next subsection. In Ref. 28, the ionization energies calculated by the 2ph-TDA (Tamm-Dancoff approximation) have been reported for $Mo(CO)_6$ and $W(CO)_6$. The 2ph-TDA improved the OVGf ionization energies in higher energy region. The TDA results are shown in Tables III and IV. Only the energy values have been given in Ref. 28 without the irreducible representation or character of states. Therefore, the correspondence of the SAC-CI results with the TDA energies was not ensured.

For $W(CO)_6$, the DKS results were similar to our results in relative values; however, the absolute values by the DKS

TABLE V. Ionization energies (IE in eV) and intensities (I) of metal hexacarbonyls including shake-up satellite states.

Cr(CO) ₆ (opt geom) ^a			Mo(CO) ₆ (opt geom) ^a			W(CO) ₆ (opt geom) ^a			Cr(CO) ₆ (exp geom) ^b		
	IE	I		IE	I		IE	I		IE	I
T _{2g}	8.59	0.43	T _{2g}	8.47	0.45	T _{2g}	8.29	0.45	T _{2g}	8.24	0.42
T _{1u}	13.77	0.40	T _{1u}	13.60	0.41	T _{1u}	13.64	0.41	T _{1u}	13.79	0.40
T _{1g}	14.59	0.37	T _{1g}	14.46	0.37	T _{1g}	14.39	0.37	E _g	14.56	0.40
E _g	14.81	0.41		19.31	0.004		19.42	0.005	T _{1g}	14.62	0.37
T _{2u}	14.84	0.37		19.96	0.002	T _{2u}	14.59	0.36	T _{2u}	14.84	0.37
	20.48	0.0004	T _{2u}	14.62	0.37		18.55	0.004		20.20	0.005
T _{2g}	15.48	0.37		18.87	0.005		19.82	0.002	T _{2g}	15.38	0.36
	19.26	0.009	T _{1u}	14.93	0.37	T _{1u}	14.86	0.37		18.85	0.010
T _{1u}	15.49	0.37		18.90	0.006		18.60	0.004	T _{1u}	15.40	0.37
	20.48	0.005	T _{2g}	15.06	0.36		19.74	0.002		20.20	0.005
A _{1g}	16.19	0.38		18.55	0.003	T _{2g}	14.99	0.36	A _{1g}	16.12	0.38
E _g	18.06	0.37		19.00	0.002		19.01	0.002	E _g	17.94	0.19
	19.01	0.004		19.15	0.004		19.29	0.005		18.09	0.18
T _{1u}	18.29	0.37		19.70	0.003		19.81	0.002	T _{1u}	18.19	0.37
A _{1g}	19.90	0.36	E _g	15.10	0.40	E _g	15.11	0.40	A _{1g}	19.60	0.36
				18.20	0.059	A _{1g}	15.88	0.38			
			A _{1g}	15.65	0.38	T _{1u}	17.98	0.37			
			T _{1u}	17.97	0.37	E _g	18.16	0.38			
			E _g	18.03	0.32	A _{1g}	19.25	0.37			
			A _{1g}	18.94	0.37		20.06	0.002			

^aCalculated with the CCSD(T) optimized geometry.^bCalculated with the neutron diffraction geometry (Ref. 43).

method were underestimated and could not be compared directly with the experimental findings. The SO effects are small in the ionization spectra of Cr(CO)₆ and Mo(CO)₆; therefore, we can discuss the assignment of spectra without the SO effect. However, the SO splitting is significant for some states of W(CO)₆. We will discuss the ionization of the molecules mainly without the SO effect and will consider the effect of SO on the states if it is important.

The valence ionizations of these carbonyls have been classified into three regions: region A around 8.5 eV, region B at 13–17 eV, and region C at 17–20 eV.²⁰ The nature of the ionization has been roughly considered as follows. Region A is the ionization from metal d orbitals, region B is the ionization from the CO outer-valence 1π and 5σ orbitals, and region C is the ionization from the CO inner-valence 4σ orbital. The character of the metal orbitals showed mixing with the ligand σ orbital.

The single peak in region A was unambiguously assigned to the 1²T_{2g} state for all three carbonyls. This state involving ionization of the valence d electron of the metal includes the character of CO(π*) with the back-donation mechanism of the metal-ligand bond.¹⁸ The state is split into two by the SO effect; the calculated SO splits of Cr(CO)₆, Mo(CO)₆, and W(CO)₆ were 0.04, 0.08, and 0.23 eV, respectively. For W(CO)₆, the SAC-CI result agrees well with the experimental value of 0.26 eV and also the DKS result.

Complex overlapping structures were observed in region B using PES. Based on Koopmans' theorem, Higginson *et al.*²¹ identified seven peaks in this region; however, their assignment involved uncertainties. Other studies identified only three or four peaks in this region.^{22,23} The SAC-CI spectrum in Figs. 1–3 indicated four or five peaks in this region with this FWHM. We consistently assigned the experimen-

tally identified peaks based on the SAC-CI results, although we needed to consider molecular vibrations and the higher-order contributions to the ionization cross section for more accurate simulation of the spectra.

We assigned the experimentally identified peaks of the He I PES of Cr(CO)₆ except for peaks B₄ and B₇, which were not well defined by the experiment. Peak B₁ observed at 13.38 eV was clearly assigned to the 1²T_{1u} state calculated at 13.77 eV by the SAC-CI method. Peak B₂ observed at 14.21 eV could be assigned to the 1²T_{1g} state calculated at 14.59 eV. Then, peak B₃ observed at 14.21 eV was assigned to the 1²E_g and 1²T_{2u} states calculated at 14.81 and 14.84 eV. Next we noted peak B₆ observed at 15.60 eV. This peak had to be the 1²A_{1g} state calculated at 16.19 eV because the PIES strongly supported the CO(σ) character of this state, even though the SAC-CI result seemed to be too high. When peak B₆ was assigned to the 1²A_{1g} state, there was no state that corresponds to B₇, the weak point of inflection. Therefore, the point of inflection may result from vibrations. The remaining peak B₅ was assigned to 2²T_{1u} and 2²T_{2g}. In this region, the calculated relative ionization energies agreed well with the experiment, although the absolute values were 0.4 eV higher than the experiment.

For Mo(CO)₆, peaks in region B were assigned in a similar manner to Cr(CO)₆. Obviously, peak B₁ was the 1²T_{1u} state. Peaks B₂, B₃, and B₄ could be assigned to the 1²T_{1g}, 1²T_{2u}, and 2²T_{1u} states, respectively. For these peaks, the calculated relative ionization energies agreed very well with the experiment, although the absolute values were 0.28 eV higher than the experiment. Accepting the PIES

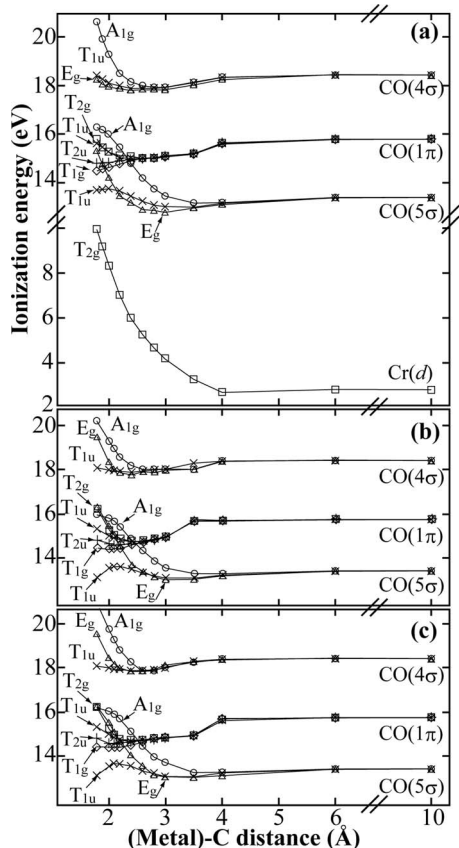


FIG. 4. Ionization energies of $M(\text{CO})_6$ with various metal-CO distances (a) $\text{Cr}(\text{CO})_6$ in the 2–20 eV region, (b) $\text{Mo}(\text{CO})_6$, and (c) $\text{W}(\text{CO})_6$ in the 12–20 eV region.

results,²² peak B_6 , which was observed around 15.6 eV, was assigned to the 1^2A_{1g} state. The remaining 1^2E_g and 2^2T_{2g} states corresponded to peak B_5 .

For $\text{W}(\text{CO})_6$, the SO effect is significant for the 2^2T_{1u} states because of the character of the 6p orbital of W that is mixing. The calculated splitting of 0.83 eV seems an overestimation of the SO effect by comparison with the DKS result. The configuration space for the SO matrix used in this study is insufficient for an accurate description of the 6p orbitals. The 1^2T_{1u} state split into $G_{3/2}^-$ and $E_{1/2}^-$ states and peak B_1 was clearly assigned to the $1G_{3/2}^-$ state. The $1E_{1/2}^-$ state has not been observed by experiment, probably because the peak is covered by the vibration of the $1G_{3/2}^-$ state. Peaks B_2 and B_3 could be assigned to the 1^2T_{1g} and 1^2T_{2u} states, respectively; the SO splittings of these states were negligible. In agreement with the PIES results, peak B_6 observed at 15.54 eV was assigned to the 1^2A_{1g} state. The assignment of the remaining two peaks was not very clear because the spectrum shape was affected by the SO splitting of the 2^2T_{1u} state that might be overestimated in the present calculation. According to the present results, peak B_4 could be assigned to the $3G_{3/2}^-$, $2E_{5/2}^+$, and $3G_{3/2}^+$ states calculated around 14.8–15.0 eV. Then, peak B_5 could be assigned to the $2E_{1/2}^-$ and $4G_{3/2}^+$ states.

In region C, two weak, broadbands were observed using He I PES. For $\text{Cr}(\text{CO})_6$, peak C_1 was assigned to the 2^2E_g and 3^2T_{1u} states, and peak C_2 was assigned to the 2^2A_{1g} state. The SAC-CI results were about 0.2 eV higher than the

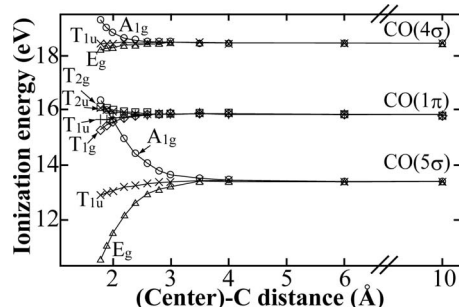


FIG. 5. Ionization energies of $(\text{CO})_6$ in O_h geometry with various center-CO distances.

experimental findings. For $\text{Mo}(\text{CO})_6$, peak C_1 was assigned to the 2^2E_g and 3^2T_{1u} states. If we assign the 2^2A_{1g} state to peak C_2 , the deviation between the SAC-CI calculation and observation is 0.76 eV. This deviation seems to be too large. The calculated ionization energy of 18.94 eV is reasonable compared with the corresponding energy for $\text{Cr}(\text{CO})_6$ because the character of this state involves the $\text{Mo}(5s)$ or $\text{Cr}(4s)$ electron; the ionization energy of $\text{Mo}(5s)$ is about 1 eV lower than that of $\text{Cr}(4s)$.²⁹ We assume that the assignment of peak C_2 to the 2^2A_{1g} state is wrong. Peak C_2 may be a shake-up state, as has been observed in $\text{W}(\text{CO})_6$.

For $\text{W}(\text{CO})_6$, four peaks were identified by SRPES.²⁴ The peaks 6 and 6' correspond to peak C_1 of the He II PES. Peak 7 was identified by SRPES and the broad peak S corresponds to peak C_2 . The peaks 6, 6', and 7 compose one broad region. These peaks were assigned to the $4G_{3/2}^-$, $3E_{1/2}^-$, and $5G_{3/2}^+$ states. Peak S could be a shake-up peak and this broad peak could contain the 2^2A_{1g} state. The calculated shake-up satellite states are shown in Table V. In the region more than 19 eV, many satellite states were calculated; therefore, peak C_2 of $\text{Cr}(\text{CO})_6$ and $\text{Mo}(\text{CO})_6$ contains the character of a shake-up peak.

B. Interaction between the metal and carbonyls

The ionization energies and the ionization character depend on the interaction between the metal and carbonyls. To illustrate this dependence, ionization energies were calculated varying the metal-CO distances. In these calculations, all metal-CO distances were changed equally to retain O_h symmetry with fixed C–O distances. The SO effect was not considered here.

The results for $\text{Cr}(\text{CO})_6$ are shown in Fig. 4(a). The eleven states resolve into four states in the long distance region where the effect of interactions is negligible. These four states are ionization of the metal valence d electron, valence 5σ , valence 1π , and inner-valence 4σ of carbonyls. Figures 4(b) and 4(c) show the states with ionization energies higher than 12 eV for $\text{Mo}(\text{CO})_6$ and $\text{W}(\text{CO})_6$. The three carbonyls show a similar dependence of ionization energies on the metal-CO distance.

The same calculations for six carbonyls in O_h geometry without a metal were carried out to study the interactions between the carbonyls. Figure 5 shows the result. The variations in ionization energy by changing the center-CO distances reflect the effect of the interaction on the ionizing

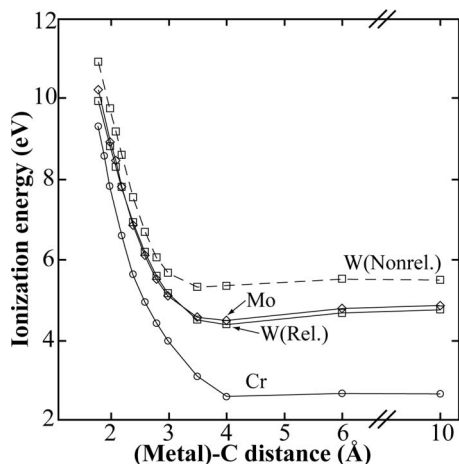


FIG. 6. The lowest ionization energies of $M(\text{CO})_6$, with various metal-CO distances with relativistic (Rel.) and nonrelativistic (Nonrel.) calculations.

electron. Ionization energies of the valence 5σ change significantly at distances below 3 Å because the ionizing electron distributes in the center-CO direction. Ionization energies of valence 1π and inner-valence 4σ show little change even at short distances because the interactions between the carbonyls have little effect on these electrons. The $\text{CO}(5\sigma)$ electrons form a bond with the metal by the σ -donation mechanism. The bond formation stabilizes the energy level of the electron and the ionization energy increases. The ionized states originating in the $\text{CO}(5\sigma)$ and $\text{CO}(1\pi)$ electrons are concentrated in the region 14–17 eV when molecules take the equilibrium geometry. Consequently, these states are observed as complex overlapping peaks in the ionization spectra. The difference in spectra between the metal carbonyls mainly depends on the metal-CO distances. The bond distance affects the relative position of the 1^2E_g state. In $\text{Cr}(\text{CO})_6$, the 1^2E_g state is the fourth lowest state but it is the seventh lowest state in $\text{Mo}(\text{CO})_6$ and $\text{W}(\text{CO})_6$.

The ionization energies of the lowest 2^2T_{2g} states are shown in Fig. 6. In the dissociation limit, these states correspond to the ionization of valence d electrons of the metals. Since they are the ionization from the closed-shell singlet to doublet, they are not the ionization of bare metal atoms in their ground state. They are highly excited state of metal atoms but corresponding experimental data have not been available. In bonding region, the valence d electrons form the bond with carbonyls by the π back-donation mechanism,¹⁸ and these states are the ionization of these bonding electrons. Formation of the bond increases the ionization energy in the region below 4 Å because the bond formation stabilizes the energy level of the valence electrons. The ionization energy curves of the three carbonyls show a similar trend. In particular, those of $\text{Mo}(\text{CO})_6$ and $\text{W}(\text{CO})_6$ are approximately the same. The result that the 2^2T_{2g} states of $\text{Mo}(\text{CO})_6$ and $\text{W}(\text{CO})_6$ have approximately the same ionization energies at the same bond distance is caused by the relativistic effect. To study the relativistic effect, nonrelativistic calculations were also performed. The nonrelativistic results for $\text{W}(\text{CO})_6$ are shown in Fig. 6; the relativistic effects on $\text{Cr}(\text{CO})_6$ and $\text{Mo}(\text{CO})_6$ were negligible.

TABLE VI. Ionization energies (eV) of metal atoms in the closed-shell singlet state, which corresponds to the dissociation limit of $M(\text{CO})_6$.

	Cr	Mo	W
Relativistic	2.39	4.87	4.78
Nonrelativistic	2.42	4.81	5.51

C. Periodic trend of the ionization energies

The relativistic and nonrelativistic ionization energies of atoms in the closed-shell singlet state that corresponds to the dissociation limit of 1^2T_{2g} state are shown in Table VI. The ionization energy increases as the metal becomes heavier. We note that this ionization energy is not the ionization of the atomic ground state in high spin. Therefore, this closed-shell singlet state is unstable by the exchange terms because of the Pauli principle. This destabilization is largest in Cr because the spatial extent of the electrons is small. Because ionization partially eliminates this destabilization, Cr tends to be ionized more easily than the heavier atoms.

The relativistic effect diminishes the ionization energy of $\text{W}(\text{CO})_6$. As a result, $\text{Mo}(\text{CO})_6$ and $\text{W}(\text{CO})_6$ have almost the same ionization energy. The valence 5d electrons of W are destabilized by the relativistic effect because the effective nuclear potential of the 5d electrons is more efficiently screened because of the relativistic contraction of the inner electrons.⁵⁰ The relativistic effects on Cr and Mo are 0.06 eV or less but the effect on W is 0.73 eV for the atoms in the closed-shell singlet state.

Approximately the same ionization energies were observed by spectroscopy for the three metal carbonyls; the energies are about 8.1–8.5 eV. This finding is explained by the interaction between metal and carbonyls and the relativistic effect. These effects on the ionization energies are shown in Fig. 7. The magnitude of the ionization energy of the valence d electron of the metals is $\text{Cr} < \text{Mo} < \text{W}$ in the closed-shell singlet state, which corresponds to the dissociation limit at the nonrelativistic level. The formation of a carbonyl molecule increases the ionization energy. If we assume the same metal-CO distance for the three carbonyls [for example, we assumed 2.08 Å from the $\text{Mo}(\text{CO})_6$ geometry], large differences of 1 eV or more still exist between the

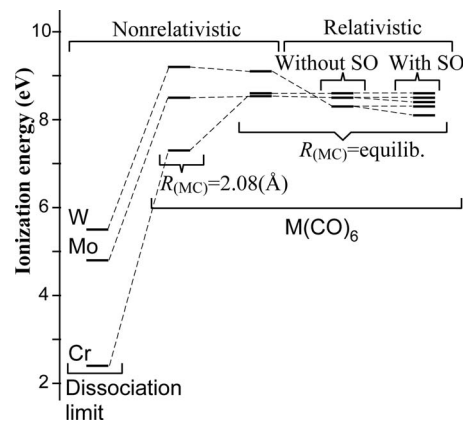


FIG. 7. The bond formation and relativistic effects on the ionization energies of $M(\text{CO})_6$.

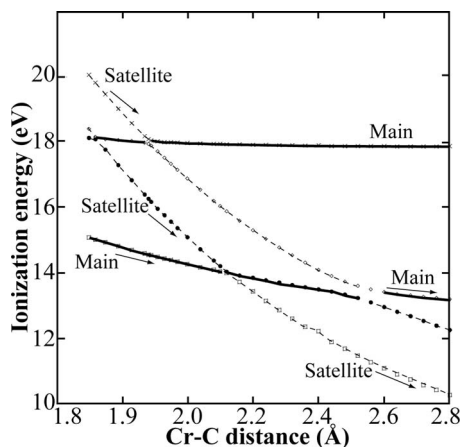


FIG. 8. Ionization energies of main and satellite E_g states for $\text{Cr}(\text{CO})_6$ with various Cr-C distances.

ionization energies of the three carbonyls. At the equilibrium geometry, the ionization energy of $\text{Cr}(\text{CO})_6$ significantly increases because the equilibrium distance of $\text{Cr}(\text{CO})_6$ is shorter than those of $\text{Mo}(\text{CO})_6$ and $\text{W}(\text{CO})_6$. As a result, the interaction between Cr and carbonyls becomes strong and the stabilization of the energy level as a result of forming the molecule is the largest. The relativistic effects decrease the ionization energy of $\text{W}(\text{CO})_6$ by about 1 eV. The SO effect splits the states but its effect on the energy is small. The short Cr-CO distance and the relativistic effect on $\text{W}(\text{CO})_6$ are the reasons why the lowest ionization energies of the three carbonyls are approximately the same.

D. Satellite states

Table V shows the main and satellite states calculated by the SAC-CI SD-R method; the states with intensity larger than 0.002 are shown. The results of main peaks in Table V with the CCSD(T) optimized geometry are identical with the results in Tables II-IV. In the SAC-CI calculations with the CCSD(T) optimized geometry, the satellite states have only hundred times smaller intensity than the main states; therefore, the distinction between the main and satellite states is obvious. The satellite states appeared in energy region more than 18 eV. Since the relative intensity was small, the satellite states had little effect on the shapes of spectrum less than 19 eV. The satellite states had some effect on the spectrum in 19–20 eV because they were dense in higher than 19 eV.

Satellite states which have as large intensity as main states were not calculated by the SAC-CI method; such states have been reported by the ADC(3) calculation of $\text{Cr}(\text{CO})_6$ in $2E_g$ and $3T_{1u}$ states.²⁷ We also performed the SAC-CI calculation of $\text{Cr}(\text{CO})_6$ with the neutron diffraction geometry;⁴⁵ the results are also shown in Table V. Using this geometry, the $2E_g$ state were split into two states in 17.94 and 18.09 eV with intensity 0.19 and 0.18. This split would be the same as the previous result of ADC(3) calculation.

To investigate the geometry dependence of main and satellite states, we performed the SAC-CI calculations of E_g states with various Cr-CO distances. The results are shown in Fig. 8. The geometry dependence of ionization energies in shake-up satellite states was larger than those in main states.

Avoided crossing of main and satellite states was observed around 1.94 Å. Around this bond length, these two states had similar character and almost the same intensity. It was impossible to draw a distinction between main and satellite states. It should be interpreted as a split of main state into two quasidegenerate states. The similar splitting in T_{1u} that has been reported by the ADC(3) calculation was not found out by the present SAC-CI calculations. Other factors than Cr-CO bond length may affect this T_{1u} state.

This split of peak did not affect the spectrum shape because the total intensity of main and satellite peaks did not depend on geometry. Although it broadens peaks, the effect must couple with molecular vibrations for realistic system. Discussion based only on electronic states is insufficient for this kind of quasidegenerate states. Moreover, the present calculations that include only SD would be insufficient for such situation to make reliable discussion. Thus, we do not make intensive discussion about shake-up satellite states here. We can conclude that the valence ionization spectra less than 19 eV can be studied by the SAC-CI SD-R method with including main peaks in which one-electron ionization from SAC neutral state is dominant with using the CCSD(T) optimized geometry.

IV. CONCLUSIONS

We have applied the SAC-CI method to the valence ionization spectra of group six metal hexacarbonyls up to 20 eV. The present calculations well reproduced the experimental spectra observed by He I PES, SRPES, and XPES. This study demonstrated that SAC-CI calculations apply to ionizations of typical transition metal compounds. For these types of molecules, the coupling between the orbital relaxation and electron correlation is important. This coupling is described with the unlinked terms in the SAC-CI method; therefore, the terms containing S_1 operators must be considered, as shown in the computational method of this study.

The first ionization around 8.4 eV was well reproduced by the SAC-CI method for the three carbonyls including the SO splitting observed in $\text{W}(\text{CO})_6$. The ionization in the 13–17 eV region was calculated to be about 0.2 to 0.4 eV higher than the observations. In this region, consistent assignments could be provided for the experimentally identified peaks using the SAC-CI calculations. The SO effects on the T_{1u} states were significant for $\text{W}(\text{CO})_6$ because these states involve 6p orbitals of W. In the 18–20 eV region, room for further theoretical studies remains for reliable assignments because there is the probability of observing the lowest shake-up states around 20 eV.

The ionization character could be roughly explained as the ionization of CO and d electrons of the metal; however, the interaction between CO and the metal significantly affects the ionization energies and breaks a picture as ionizations from single natural orbital. The ionizations of $\text{CO}(5\sigma)$ interact with the metal by the sigma-donation mechanism. The interaction increases these ionization energies. Consequently, the states with the origin in $\text{CO}(5\sigma)$ and $\text{CO}(1\pi)$ have energies of around 13–17 eV. Thus, many overlapping

peaks are observed in this region. The ionization energies of E_g and A_{1g} states were sensitively affected on the metal-CO bond length.

The present calculations can explain the very similar values of the first ionization energies that are observed for the three metal carbonyls. The relativistic effect diminishes the ionization energy of $W(CO)_6$ and the interaction between carbonyls and the metal increases the ionization energy of $Cr(CO)_6$. Thus, the three carbonyls have their first ionization energies around 8.4 eV.

ACKNOWLEDGMENTS

This work has been partially financially supported by a Grant for Creative Scientific Research (14GS0217) from the Ministry of Education, Culture, Sports, Science and Technology of Japan. The computations were performed using the Research Center for Computational Science, Okazaki, Japan.

- ¹ K. Kumura, S. Katsumata, Y. Achiba, T. Yamazaki, and S. Iwata, *Handbook of HeI Photoelectron Spectra of Fundamental Organic Molecules* (Japan Scientific Society, Tokyo, 1981).
- ² E. Siska, *Rev. Mod. Phys.* **65**, 337 (1993); Y. Harada, S. Masuda, and H. Ozaki, *Chem. Rev.* **97**, 1897 (1997).
- ³ T. Koopmans, *Physica* **1**, 104 (1934).
- ⁴ A. Veillard and J. Demuynck, *Modern Theoretical Chemistry*, edited by H. F. Schaefer III (Plenum, New York, 1977), Vol. 4, pp. 187–222; M. C. Böhm, *J. Chem. Phys.* **78**, 7044 (1983).
- ⁵ K. Ishimura, M. Hada, and H. Nakatsuji, *J. Chem. Phys.* **117**, 6533 (2002).
- ⁶ H. Nakatsuji and K. Hirao, *J. Chem. Phys.* **68**, 2053 (1978).
- ⁷ H. Nakatsuji, *Chem. Phys. Lett.* **59**, 362 (1978); **67**, 329 (1979); **67**, 334 (1979).
- ⁸ H. Nakatsuji, *Acta Chir. Hung.* **129**, 719 (1992); H. Nakatsuji, *Computational Chemistry: Reviews of Current Trends*, edited by J. Leszczynski (World Scientific, Singapore, 1997), Vol. 2, pp. 62–124; M. Ehara, M. Ishida, K. Toyota, and H. Nakatsuji, *Reviews of Modern Quantum Chemistry: A Celebration of the Contributions of Robert G. Parr*, edited by K. D. Sen (World Scientific, Singapore, 2002), pp. 293–319; M. Ehara, J. Hasegawa, and H. Nakatsuji, *Theory and Application of Computational Chemistry: The First 40 Years*, edited by C. E. Dykstra, G. Frenking, K. S. Kim, and G. E. Scuseria (Elsevier, Oxford, 2005), Chap. 39, pp. 1099–1141; J. Hasegawa and H. Nakatsuji, *Radiation Induced Molecular Phenomena in Nucleic Acid: A Comprehensive Theoretical and Experimental Analysis*, edited by M. Shukla and J. Leszczynski, (Springer, Dordrecht, Netherlands, 2008) Chap. 4, pp. 93–124.
- ⁹ O. Kitao and H. Nakatsuji, *J. Chem. Phys.* **87**, 1169 (1987); J. Wan, M. Ehara, M. Hada, and H. Nakatsuji, *ibid.* **113**, 5245 (2000); J. Wan, M. Hada, M. Ehara, and H. Nakatsuji, *ibid.* **114**, 5117 (2001); H. Nakatsuji, M. Komori, and O. Kitao, *Chem. Phys. Lett.* **142**, 446 (1987); M. Ehara, M. Nakata, and H. Nakatsuji, *Mol. Phys.* **104**, 971 (2006).
- ¹⁰ P. Tomasello, J. Hasegawa, and H. Nakatsuji, *Europhys. Lett.* **41**, 611 (1998); M. Ehara, Y. Ohtsuka, and H. Nakatsuji, *Chem. Phys.* **226**, 113 (1998); P. Tomasello, M. Ehara, and H. Nakatsuji, *J. Chem. Phys.* **118**, 5811 (2003).
- ¹¹ H. A. Fogarty, H. Tsuji, D. E. David, C.-H. Ottosson, M. Ehara, H. Nakatsuji, K. Tamao, and J. Michl, *J. Phys. Chem. A* **106**, 2369 (2002).
- ¹² M. Ehara, S. Fukawa, H. Nakatsuji, D. David, E. Z. Pinkhassik, M. Apostol, and J. Michl, *Chem. Asian J.* **2**, 1007 (2007).
- ¹³ H. Nakatsuji, *Chem. Phys. Lett.* **177**, 331 (1991).
- ¹⁴ M. Ehara and H. Nakatsuji, *Chem. Phys. Lett.* **282**, 347 (1998); J. Hasegawa, M. Ehara, and H. Nakatsuji, *Chem. Phys.* **230**, 23 (1998); M. Ehara and H. Nakatsuji, *Spectrochim. Acta, Part A* **55**, 487 (1999); M. Ehara, P. Tomasello, J. Hasegawa, and H. Nakatsuji, *Theor. Chem. Acc.* **102**, 161 (1999); M. Ehara, M. Ishida, and H. Nakatsuji, *J. Chem. Phys.* **114**, 8990 (2001); M. Ishida, M. Ehara, and H. Nakatsuji, *ibid.* **116**, 1934 (2002).
- ¹⁵ M. Ehara, M. Ishida, and H. Nakatsuji, *J. Chem. Phys.* **117**, 3248 (2002); M. Ehara, Y. Ohtsuka, H. Nakatsuji, M. Takahashi, and Y. Udagawa, *ibid.* **122**, 234319 (2005); M. Ehara, S. Yasuda, and H. Nakatsuji, *Z. Phys. Chem.* **217**, 161 (2003).
- ¹⁶ M. Ehara, M. Ishida, and H. Nakatsuji, *Collect. Czech. Chem. Commun.* **70**, 881 (2005).
- ¹⁷ H. Nakatsuji and S. Saito, *Int. J. Quantum Chem.* **39**, 93 (1991); H. Nakatsuji, M. Ehara, M. H. Palmer, and M. F. Guest, *J. Chem. Phys.* **97**, 2561 (1992); H. Morita, H. Nakai, P. Tomasello, and H. Nakatsuji, *Bull. Chem. Soc. Jpn.* **69**, 1893 (1996).
- ¹⁸ N. A. Beach and H. B. Gray, *J. Am. Chem. Soc.* **90**, 5713 (1968).
- ¹⁹ E. R. Davidson, K. L. Kunze, F. B. C. Machado, and S. H. Chakravorty, *Acc. Chem. Res.* **26**, 628 (1993).
- ²⁰ E. W. Plummer, W. R. Salaneck, and J. S. Miller, *Phys. Rev. B* **18**, 1673 (1978); J. L. Pascual, L. G. M. Pettersson, and H. Ågren, *ibid.* **56**, 7716 (1997).
- ²¹ B. R. Higginson, D. R. Lloyd, P. Burroughs, D. M. Gibson, and A. F. Orchard, *J. Chem. Soc., Faraday Trans. 2* **69**, 1659 (1973).
- ²² A. Nilsson, N. Mårtensson, S. Svensson, L. Karisson, D. Nordfors, U. Gelius, and H. Ågren, *J. Chem. Phys.* **96**, 8770 (1992).
- ²³ G. Cooper, J. C. Green, M. P. Payne, B. R. Dobson, and I. H. Hillier, *J. Am. Chem. Soc.* **109**, 3836 (1987).
- ²⁴ Y.-F. Hu, G. M. Bancroft, Z. Liu, and K. H. Tan, *Inorg. Chem.* **34**, 3716 (1995).
- ²⁵ S. Masuda and Y. Harada, *J. Chem. Phys.* **96**, 2469 (1992).
- ²⁶ C. S. Nash and B. E. Bursten, *New J. Chem.* **19**, 669 (1995).
- ²⁷ M. Ohno, W. von Niessen, and F. Tarantelli, *Phys. Rev. B* **45**, 1851 (1992).
- ²⁸ C. A. Bayse and K. N. Ortwine, *J. Phys. Chem. A* **111**, 7841 (2007).
- ²⁹ C. E. Moore, *Atomic Energy Levels* (National Bureau of Standards, Washington, 1971) Vols. II and III.
- ³⁰ Y.-J. Chen, C.-L. Lian, and C. Y. Ng, *J. Chem. Phys.* **107**, 4527 (1997).
- ³¹ J. Rolke, Y. Zheng, C. E. Brion, S. J. Chakravorty, E. R. Davidson, and I. E. McCarthy, *Chem. Phys.* **215**, 191 (1997).
- ³² R. Fukuda and H. Nakatsuji, *J. Chem. Phys.* **128**, 094105 (2008).
- ³³ M. J. Frisch, G. W. Trucks, H. B. Schlegel *et al.*, GAUSSIAN Development Version, Revision E.05, Gaussian Inc., Wallingford, CT, 2006.
- ³⁴ H. Nakatsuji, M. Hada, M. Ehara, K. Toyota, R. Fukuda, J. Hasegawa, M. Ishida, T. Nakajima, Y. Honda, O. Kitao, and H. Nakai, SAC-CI GUIDE (2005). (PDF file is available at <http://www.qcri.or.jp/sacci/>).
- ³⁵ M. Douglas and N. M. Kroll, *Ann. Phys. (N.Y.)* **82**, 89 (1974); B. A. Hess, *Phys. Rev. A* **32**, 756 (1985); **33**, 3742 (1986).
- ³⁶ A. Schafer, C. Huber, and R. Ahlrichs, *J. Chem. Phys.* **100**, 5829 (1994).
- ³⁷ K. G. Dyall, *Theor. Chem. Acc.* **117**, 483 (2007).
- ³⁸ K. G. Dyall, *Theor. Chem. Acc.* **112**, 403 (2004).
- ³⁹ T. H. Dunning, Jr. and P. J. Hay, in *Modern Theoretical Chemistry*, edited by H. F. Schaefer III (Plenum, New York, 1977), Vol. 3, pp. 1–27.
- ⁴⁰ A. W. Ehlers and G. Frenking, *J. Am. Chem. Soc.* **116**, 1514 (1994).
- ⁴¹ A. Rosa, E. J. Baerends, S. J. A. van Gisbergen, E. van Lenthe, J. A. Groeneveld, and J. G. Snijders, *J. Am. Chem. Soc.* **121**, 10356 (1999).
- ⁴² Y. Ishikawa and K. Kawakami, *J. Phys. Chem. A* **111**, 9940 (2007).
- ⁴³ A. Jost, B. Rees, and W. B. Yelon, *Acta Crystallogr., Sect. B: Struct. Crystallogr. Cryst. Chem.* **31**, 2649 (1975).
- ⁴⁴ B. Rees and A. Mitschler, *J. Am. Chem. Soc.* **98**, 7918 (1976).
- ⁴⁵ S. V. Arnesen and H. M. Seip, *Acta Chem. Scand.* **20**, 2711 (1966).
- ⁴⁶ T. C. W. Mak, *Z. Kristallogr.* **166**, 277 (1984).
- ⁴⁷ H. Nakatsuji, *Chem. Phys.* **75**, 425 (1983); H. Nakatsuji, J. Hasegawa, and M. Hada, *J. Chem. Phys.* **104**, 2321 (1996).
- ⁴⁸ S. Suzer, S. T. Lee, and D. A. Shirley, *Phys. Rev. A* **13**, 1842 (1976); R. I. Martin and D. A. Shirley, *J. Chem. Phys.* **64**, 3685 (1976).
- ⁴⁹ T. Nakajima and K. Hirao, *J. Chem. Phys.* **121**, 3438 (2004).
- ⁵⁰ P. Pykkö, *Chem. Rev.* **88**, 563 (1988).